Eddy-resolving Simulation of the World Ocean Circulation by using MOM3-based OGCM Code (OFES) Optimized for the Earth Simulator

Group Representative
Hideharu Sasaki The Earth Simulator Center, Research Scientist

Author
Hideharu Sasaki The Earth Simulator Center, Research Scientist

The Earth Simulator enables us to perform eddy-resolving simulations on the global domain to assess simulated eddy-dynamics together with the phenomenological validations of our numerical experiments. In order to pursue this goal, we have developed a high-resolution MOM3-based OGCM code (OFES) optimized for the Earth Simulator. We have executed a fifty-year time integration of the global eddy simulation with the horizontal resolution 0.1 degree and with 54 vertical levels.

A quick look at the simulated surface currents tells that the overall characteristics of those fields are quite realistic. Well-documented meandering patterns of the Kuroshio with realistic separation latitude are readily identified. Other well-known features of the world ocean circulation such as the Gulf Stream and accompanying rings, Agulhas rings in the Agulhas Current and the herringbone structures of the Legeckis waves in the eastern tropical Pacific manifest themselves naturally in our high-resolution simulation.

Keywords: OGCM, OFES, high-resolution, mesoscale eddy

Model setting

The computational domain covers a near-global region extending from 75˚S to 75˚N except for the Arctic Ocean. The horizontal resolution and the number of vertical levels we employed are 0.1 degree and 54 respectively. The depth of first level is about 5m and the maximum depth is 6,065m. Model bottom topography is interpolated from 1/30 degree bathymetry data set created by the OCCAM project at the Southampton Oceanography Centre. The surface momentum, heat and salinity fluxes are specified from monthly mean NCEP re-analyses data in addition to a surface salinity restoring to climatological value. The model was spun up from annual mean temperature and salinity fields (WOA98) without motion. To suppress grid-scale noises, we introduced a scale-selective damping of Bi-harmonic type and employed KPP scheme for the vertical mixing.

Code optimization and computational performance

To attain high performance of our eddy resolving code, a number of different optimization techniques have been utilized considering distinctive characteristics of the Earth Simulator. First of all, each routine must be vectorized to improve the performance on vector machines. In addition, we applied such common techniques as inline expansions, loop merging, loop unrolling/rerolling together with re-ordering in order to reduce the number of calling procedures and to make the averaged length of do-loops longer. In some cases, techniques of loop fission/splitting and loop fusion are reintroduced in a balanced manner. As the first step of optimization, we attempted to make the vector ratio of almost all routines to exceed 99.5%. Attained the maximum value of averaged vector length, vector ratio and value of the total flops are indicated in Table 1, where the maximum vector length and peak performance for each processor are 256 and 8 Gflops respectively.

We employed one dimensional domain decomposition in the meridional direction, in which parallelization procedure is limited by the number of employed latitudinal circles, namely, the maximum number of CPUs to be used for a near global domain extending from 75˚S to 75˚N is 1500 provided that the meridional resolution is 0.1 deg. Each processor is assigned computation in zonal strips. The number of meridional grid points in a zonal strip depends on the number of processors. As the number of processors increases, the meridional extent of a strip becomes comparable to or smaller than a halo region. This means that some device is necessary to reduce computational burdens especially in the halo regions. It becomes more and more important to improve the parallel performance of the code. Especially, computational burden in halo regions is not reduced by simply dividing a

Table 1 Routine-wise vector length, ratio and the total flops elapsed.

Main computation [routine names]	CPU time (%)	MFLOPS	Vector Ratio	Ave. Vector Length
baroclinic computation [baroclinic]	14.3	4900.7	99.8	240.0
vertical mixing with implicitly [invtri]	13.0	3374.6	99.6	240.0
Barotropic coputation [expl_freesurf]	11.0	4902.6	99.7	240.0
unisco_density [unisco_density]	8.4	5202.2	99.8	256.0
computation with biharmonic [delseq_velocity]	7.5	4255.7	99.7	240.0
Main computation of tracers [tracer]	7.1	5025.9	99.8	240.0
calculate advection velocities [adv_vel]	4.2	4838.7	99.6	240.0
construct diagnostics [diagt1]	2.6	3801.6	99.5	243.0
computation of normalized densities [statec]	2.4	6613.0	99.8	240.1

Table 2 Scaling factor with 4 halo regions.

Total CPU		12	20	60	100	300	500	1500
MPI	Lines /CPU	129	79	29	19	9	7	5
	scaling factor	11.63	18.99	51.72	78.95	166.67	214.29	300.00
MPI + autotasking*	Lines /CPU	126	76	26	16	6	4	2
	scaling factor	11.90	19.74	57.69	93.75	250.00	375.00	750.00

* 4 parallelized for intra-node

given computation into many nodes. To this end, we employed microtasking techniques for intra-node parallelization while inter-node communications were achieved via MPI library to get the best communication performance on the Earth Simulator. Table 2 shows that computational burdens in the halo regions can be reduced by microtasking techniques. As a result of our tuning efforts, the parallel efficiency and vector ratio of our code are 99.87% and 99.52% respectively and one model-year simulation has been completed in seven hours.

Results

Simulated annual mean sea surface height distribution is shown in Figure 1. We can clearly see that, in consistent with a simple geostrophic relation, the SSH in the subtropics is higher than that in the sub-polar region and the lowest SSH appears in the southern flank of the strong Antarctic Circumpolar Current. A zonal band of lower SSH can be noticed along 7˚N in the Pacific, which corresponds to the boundary between the North Equatorial Current and the North Equatorial Countercurrent. Therefore, we can say that the basin-wide pattern of the mean SSH field is simulated well.

Smith et al. (2000) suggest that the distribution of eddy activity becomes realistic compare to that derived observation data with increasing horizontal grid spacing. Fig.2 shows the root-mean-square variation of the simulated SSH anomaly. The variability maxima appear in the western boundary current regions such as the Kuroshio/Kuroshio Extension, the Gulf Stream/the North Atlantic Current, the Malvinas Current and the Agulhas Current and around the Antarctic Circumpolar Current. For example, in the Kuroshio region, a high SSH variability region extends from Japan coast to the date line in forming a zonal band. This is mostly due to the path variation of the Kuroshio Extension (Mizuno and White,

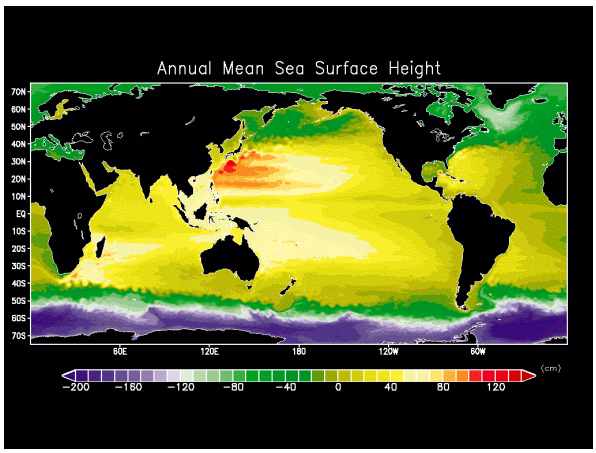

Fig. 1 Simulated annual mean sea surface height.

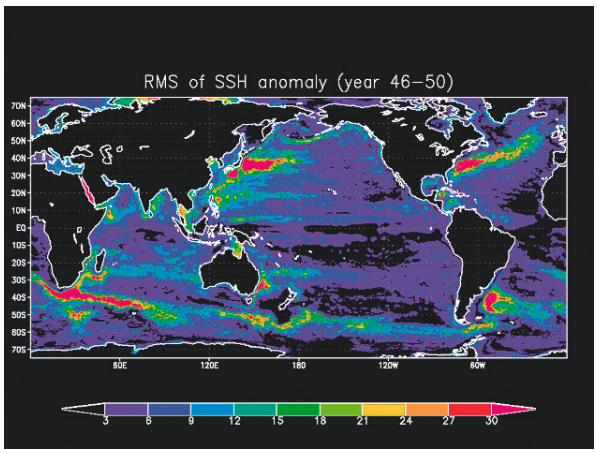

Fig. 2 Root-mean-square variation of sea surface height.

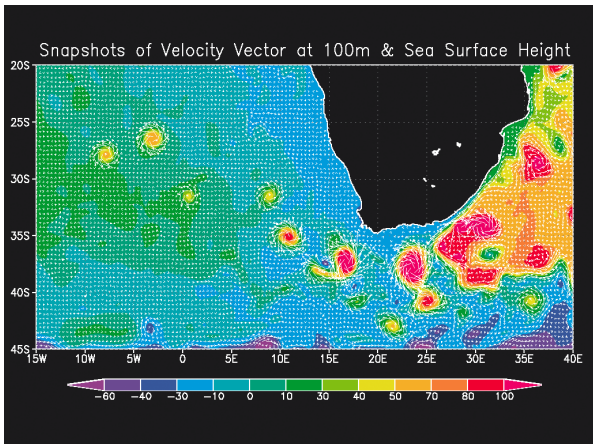

Fig. 3 Snapshot fields of sea surface height and velocity velocity vector at 100m in the south of Africa.

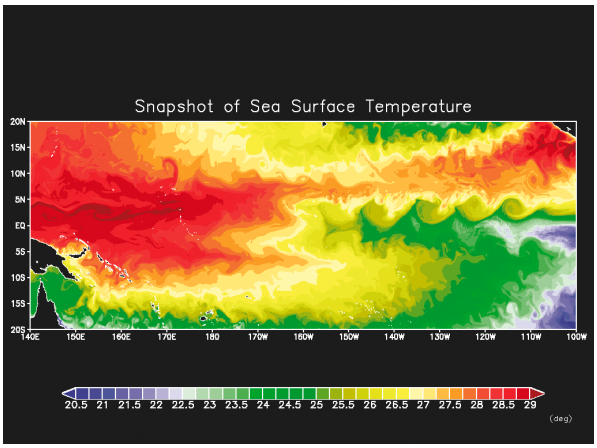

Fig. 4 Snapshot of sea surface temperature in the eastern tropical Pacific in 15 September at 50th model year.

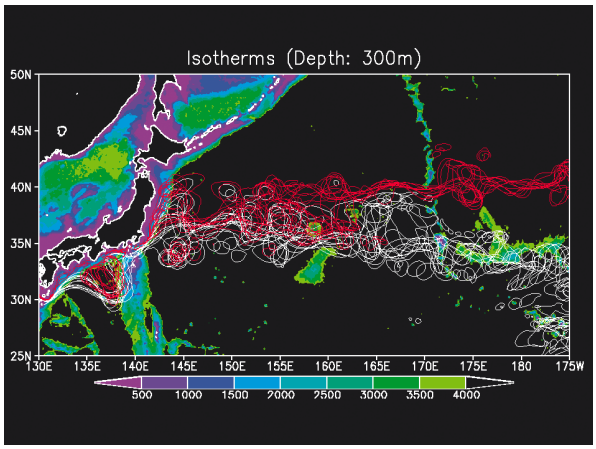

Fig. 5 Monthly-mean Kuroshio Current paths as defined by the 14˚C (Black) and 10˚C (red) isotherm at 300m depth, superimposed upon bathymetry.

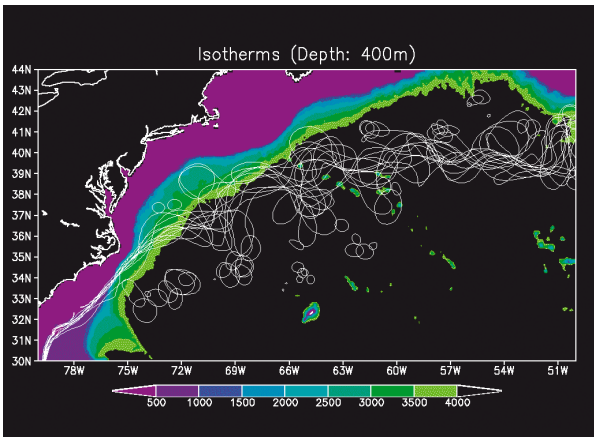

Fig. 6 Monthly-mean Gulf Stream paths as defined by the 12˚C isotherm at 400m depth, superimposed upon bathymetry.

1983). Fairly high variability regions are also seen along 20N and 6N in the western Pacific. Locations of these high variability regions are observationally confirmed by the satellite altimetry (Le Traon and Orgor, 1988).

We can see the mesoscale features of ubiquitous activities in our high-resolution simulation. Fig.3 shows the snapshot of the sea surface height and the velocity field in the south of Africa. Our model reproduce several eddies, so-called Agulhas Rings shed at the Agulhas retroflection. Agulhas Rings are anti-cyclonic eddies, which contribute to the heat transfer from Indian Ocean to Atrantic Ocean. The scale of the simulated Agulhas Rings is close to the observation. Fig.4 is the snapshot of the sea surface temperature in the eastern tropical Pacific in the fall. Legeckis waves are the meandering front structure between the cold upwelling water of the Pacific equatorial cold tongue and the warm water (Legeckis, 1977). Such tropical instability waves, which propagate westward, are simulated well in our eddy-resolving model.

It is well known that in low-resolution simulations the western boundary current tends to overshoot and the resulting separation point turns out to be quite unrealistic. The composites of the simulated monthly mean Kuroshio and Gulf Stream paths during one year are shown in Fig.5 and Fig.6. Both simulated western boundary currents separate with right latitude. And the Kuroshio Extension bifurcates into two branches. Observation (Mizuno and White, 1983) suggested that the bifurcated Kuroshio Extension is controlled by the bottom topography. The horizontal resolution of our model is enough to resolve mesoscale eddy and fine structure of bottom topography. The similarity to the observation is mainly attributed to high resolution of our model.

Summary

We have developed OGCM code (OFES) optimized for the Earth Simulator. A number of different optimization techniques are employed. As the result of our effort, we have performed fifty-year-integration of our global eddy-resolving simulation. A quick look at the simulated result tells that the

overall characteristics of oceanic fields are quite realistic. The hi-resolution of the model contributes to resolve the fine structure such as the mesoscale eddies, which encourages us to extend our investigation further on variety of topics.

Reference

Le Traon, P.-Y. and F. Ogor, 1998: ERS-1/2 orbit improvement using TOPEX/POSEIDON: The 2cm challenge, *J. Geophys Res*., 103, 8045-8057.

Legeckis, R., 1977: Long waves in the eastern tropical Pacific Ocean: A view from a geostationary satellite. *Science*, 197, 1179-1181.

Mizuno, K., and W. B. White, 1983: Annual and interannual variability in the Kuroshio current system. *J. Phys. Oceanogr*., 13, 1847-1867.

Smith, R. D., M. E. Maltrud, F. O. Bryan, and M. W. Hecht, Numerical simulation of the North Atlantic Ocean at 1/10, *J. Phys. Oceanogr*., 30, 1532-1561, 2000.

海洋大循環モデルMOM3（OFES）による超高解像度数値実験研究

利用責任者
佐々木英治　　地球シミュレータセンター 研究員
著者
佐々木英治　　地球シミュレータセンター 研究員

海洋大循環モデルは海流などの大規模の循環系と中規模渦と呼ばれる数10kmスケールの渦擾乱を同時に取り扱うことが困難であった。そこで、海洋大循環モデルMOM3を地球シミュレータ用に最適化、並列化した海洋大循環モデルOFESを開発し、海洋の中規模渦を十分に解像する水平解像度0.1度の準全球世界海洋で海洋循環のスピンアップに十分な50年間の積分を実行した。モデル結果を検証したところ、全球の中規模渦の活動分布（下図）は衛星観測データとほぼ一致し、レジキス波やアガラスリングなどの代表的な中規模渦が見られ、中規模渦に代表される変動場がモデルでよく再現されていた。また、水平解像度を高解像度にすることにより、黒潮などの西岸境界流の離岸位置が正確に再現されるなど、全球規模の海洋循環場はおおむね良好な結果となった。今後、出力された膨大なデータの詳細な解析を進めると同時に、トレーサ実験、ハインドキャスト実験を実施する予定である。

キーワード：海洋大循環モデル、OFES、中規模渦、超高解像度

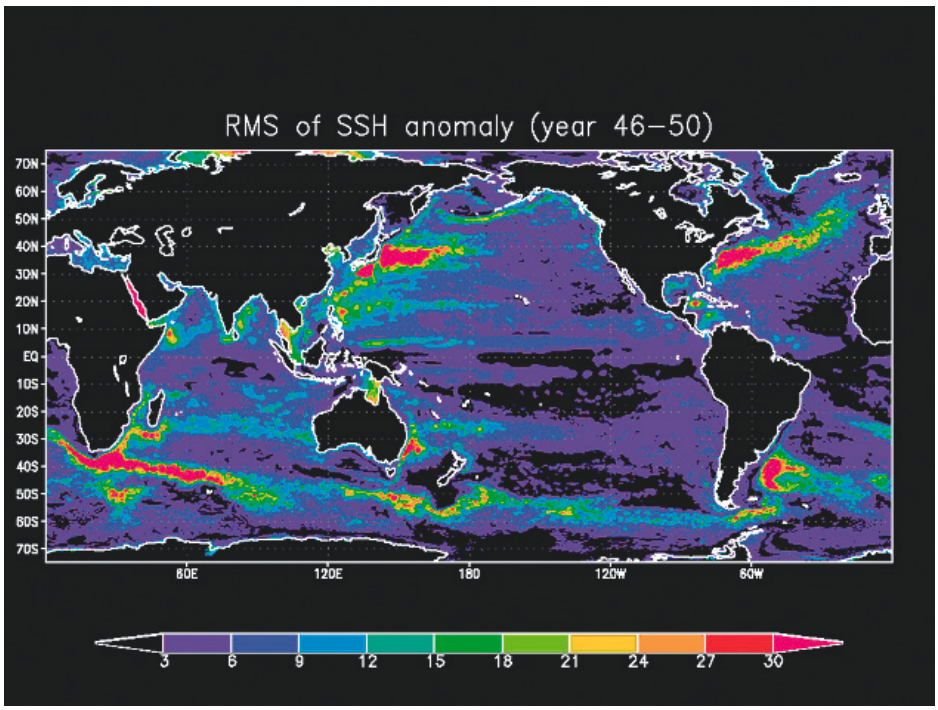

海面高度アノマリーのRMS（モデル46年～50年）